

Role of the Dinucleotide Signaling Molecule Diadenosine Tetraphosphate in *Staphylococcus aureus* Pathogenesis

Jackson Coker

Biology Department
The University of North Carolina Asheville
One University Heights
Asheville, North Carolina 28804 USA

Faculty Mentor: Dr. Melinda Grosser

Abstract

Staphylococcus aureus can cause a wide range of infections in humans from skin and soft tissue infections to more severe pneumonia, osteomyelitis, bacteremia, and endocarditis, in part aided by its ability to naturally resist the innate immune system. In addition to its pathogenicity, drug resistant strains have emerged in both community and hospital settings. The ability of methicillin-resistant *Staphylococcus aureus* (MRSA) to resist immune cell-produced nitric oxide (NO \cdot), and to effectively form antimicrobial-resistant biofilms makes it an important pathogen to study. Recently, the *S. aureus* enzyme YqeK was discovered to degrade the dinucleotide molecule, Ap₄A, which has not previously been studied in *S. aureus*. In other bacteria, elevated Ap₄A reduces antibiotic and stress resistance as well as biofilm formation. Here, we created a Δ yqeK deletion mutant in a community-acquired MRSA strain (LAC) and assessed its fitness during both NO \cdot resistance and biofilm formation. Relative to wild-type, the Δ yqeK deletion strain demonstrated a significantly decreased ability to resist NO \cdot , a decreased ability to form biofilms on polystyrene plates, and a decreased ability to form biofilms on human plasma coated plates. Future work will include RNA-sequencing to determine how gene expression differs in the Δ yqeK deletion strain in order to identify a possible mechanism for these phenotypes and further explore the potential of YqeK or Ap₄A as drug targets.

Introduction

Staphylococcus aureus is one of the most deadly and costly human pathogens in the United States (1). It is the leading cause of skin and soft tissue infections (SSTIs), in addition to acutely dangerous illnesses including bacteremia, endocarditis, osteomyelitis, and pneumonia (2). *S. aureus* is capable of resisting cell wall-targeting β -lactam antibiotics (e.g., penicillin) via the production of β -lactamases but also by encoding an alternative cell wall transpeptidase, PBP2a. PBP2a allows it to resist next generation β -lactam antibiotics including methicillin, leading to methicillin-resistant *S. aureus* (MRSA). Although historically a disease that was mostly contained within hospitals, there are now more virulent strains of MRSA infecting otherwise healthy individuals outside of hospitals. This community-acquired MRSA (CA-MRSA) speaks to the increasing dangers of *S. aureus*, coupled with the ever more prevalent antibiotic crisis. In addition to its ability to resist common antibiotics, *Staphylococcus aureus*, like other infectious pathogens, has an uncanny ability to survive stressors induced by the host.

S. aureus virulence is partially due to its ability to grow in the presence of nitric oxide (NO^\cdot), which is commonly produced by the host to inhibit bacterial and fungal invaders (3, 2). One mechanism for the antibacterial activity of NO^\cdot is the increased endogenous production of reactive oxygen species (ROS) in bacteria. These ROS interact with NO^\cdot to produce a variety of additional toxic reactive nitrogen species (RNS). At high levels, RNS inhibit bacterial respiration, in part, by selective reversible binding to bacterial metalloenzymes (heme iron, iron-sulfur clusters, and other metal cofactors) and protein thiols (4, 5). Under significant NO^\cdot stress, the cytochrome P450 heme iron is reversibly bound, preventing O_2 from binding, thus inhibiting respiration (6). Additionally, NO^\cdot and its derivatives are capable of damaging DNA, lipid peroxidation, and nitration of tyrosine residues (7). In order to continue growing during NO^\cdot stress, *S. aureus* must sense and respond to each of these problems.

An additional virulence trait of *S. aureus* is its ability to form biofilms. Biofilms are matrix-encapsulated bacterial colonies capable of growing in nearly any environment, which increase their resistance capabilities (8). Biofilm matrices are primarily composed of exopolysaccharide (EPS), which acts as a barrier against the environment and facilitates nutrient and gene transfer, as well as proteins and extracellular DNA (8). The natural resistance *S. aureus* possesses against the body's innate immune system and its ability to form biofilms on medical implants, like artificial heart valves (endocarditis), exacerbates its virulent potential.

Like many successful pathogens, *S. aureus* has a robust ability to detect environmental changes, to elicit an internal response (9). In exploring *S. aureus*' ability to respond to the infection environment, a gene was identified that may play a role NO^\cdot resistance and biofilm formation. A transposon-sequencing screen was previously performed to identify any genes required for full *S. aureus* fitness during NO^\cdot stress, in a pooled transposon mutant library (7). The gene SAUSA300_1552 was one of several hundred genes identified. In 2020, the product of this gene was determined to be an adenosine tetraphosphate (Ap_4A) hydrolase, YqeK (10).

Under oxidative stress-inducing conditions, organisms accumulate specific dinucleoside polyphosphates in significant amounts, the most common being Ap_4A (Figure 1) (11, 12, 13). Ap_4A is a common molecule across living organisms, including

humans (14). It is created from catalysis by aminoacyl tRNA synthetases (ARS) in the reverse reaction of the amino acid activation step of translation by ARS. (15). Many virulent bacteria, such as *Salmonella enterica* and *Bartonella bacilliformis*, depend on Ap₄A levels to be highly regulated by enzymatic degradation (16, 17). The degradation of diadenosine tetraphosphates is performed by a hydrolase which results in two ADP molecules. Many pathogenic bacteria possess hydrolase homologs, such as the *apaH* gene in *P. fluorescens* (18). In Gram positive bacteria that lack ApaH homologs, Ap₄A degradation was recently found to be performed by YqeK. However the importance of degradation is not fully understood, nor is the general role of Ap₄A (Figure 2) (10).

Previous studies in other bacterial species, including *Physarum polycephalum*, and *Escherichia coli*, have suggested that Ap₄A could be either a damage marker or a *bona fide* signaling molecule. During certain types of stress, it accumulates to concentrations up to 30 fold greater than concentrations under non-damaging inducing conditions (13). In the Gram positive *Streptococcus mutans*, YqeK may play a role in biofilm formation, as when the gene was deleted, *S. mutans* formed less biofilm (19). It was also found in the Gram negative *Pseudomonas fluorescens* that under conditions that lead to rising Ap₄A levels, the bacteria had a greater affinity to biofilm formation, rather than remaining planktonic (18).

Little research has been performed on the effect of Ap₄A levels, via the manipulation of YqeK, in Gram positive bacteria. Based on previous research in other pathogens, we hypothesized that without a functional YqeK, *S. aureus* would exhibit an increased susceptibility to antibiotics (which often kill by inducing oxidative stress in bacteria), an increased sensitivity to stressors, decreased pathogenicity, and a hindered ability to form biofilms (10,11). If so, this would identify YqeK as a promising new target for antibiotic drugs, or as an antibiotic adjuvant. To investigate the role of YqeK in *S. aureus*, our lab created a deletion mutant of *yqeK*. Here, we show that this deletion mutant is in fact more sensitive to NO[•] stress, and exhibits a reduced ability to form biofilms, relative to WT.

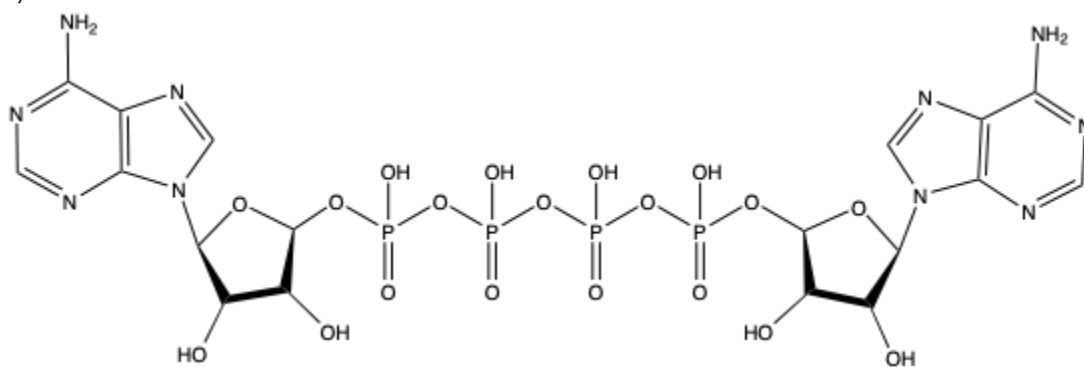


Figure 1. Structure of diadenosine tetraphosphate, Ap₄A.

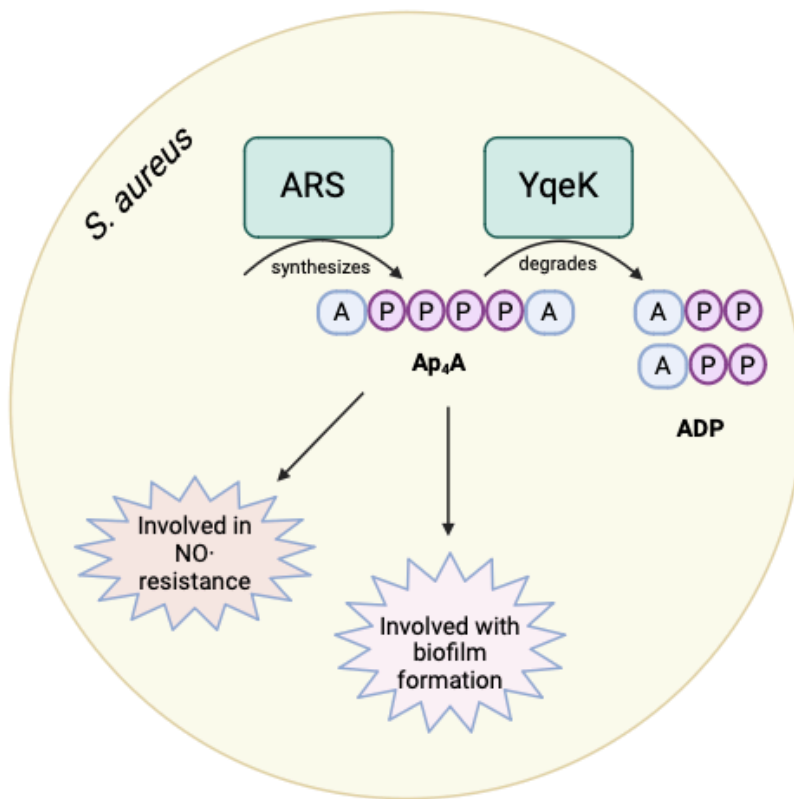


Figure 2. Diagram of the Ap₄A degradation as understood in *Staphylococcus aureus*.

Materials and Methods

2.1 Bacterial Strains and Culture Conditions

For all *S. aureus* growth experiments, we used a common lab CA-MRSA strain, LA clone (20). The LAC $\Delta yqeK$ deletion mutant used for these experiments was previously constructed and contains an in-frame deletion of the *yqeK* gene leaving behind only the start and stop codons so that transcription/translation of downstream genes in the same operon are not affected. Bacterial overnight cultures were grown in glass culture tubes containing 5 mL tryptic soy broth (TSB) for 16-20 hours, or until stationary phase, at 37°C while shaking at 250 rpm. When necessary to maintain a plasmid, the bacteria were grown under the same conditions but with the addition of 10µg/mL chloramphenicol.

2.2 NO \cdot Growth Curves

For the NO \cdot growth curves, bacterial overnight cultures were first diluted 1:10. Using a Spectronic Genesys 2 spectrophotometer, the optical density at 650 nm (OD₆₅₀) was measured. The 1:10 dilution was then further diluted to an optical density of 0.01. The bacteria were added to a 96-well polystyrene plate (200µl per well). In half the wells, 10mM of (Z)-1-[N-(2-aminoethyl)-N-(2-ammonioethyl)amino]diazene-1-ium-1,2-diolate (DETANO), an NO \cdot donor, was added. The plate was grown in Biotek Synergy HTX plate reader, while shaking at 37°, using a standard growth curve procedure where OD₆₅₀ was quantified every 15 minutes for 24 hours.

To determine differences in growth between $\Delta yqeK$ and WT, we quantified the time it took each strain to reach an OD 0.4 (early exponential phase) as an approximation of lag time. A two-way ANOVA with a sidak's multiple comparison test was performed to determine the impact of adding NO \cdot and the strain difference in time required to reach an OD .4 in R-studio.

To determine the difference in maximum growth rate between $\Delta yqeK$ and WT, maximum growth rate was quantified using the following equation: change in ln OD 650 per change in time, hours. Growth rates were calculated at fifteen minute intervals. Data analysis was performed using R-studio.

2.3 Biofilm Assay

S. aureus biofilms were grown in 96-well polystyrene plates as follows: Using a Spectronic Genesys 2 spectrophotometer measuring the OD₆₅₀, bacterial overnight cultures were diluted 1:10; then further diluted to an OD₆₅₀ of 0.005. 200 µL of the bacterial dilution were pipetted into 96-well plates. 5 mM DETANO was added to the wells to represent the natural immune response. The plates were grown in the Biotek Synergy HTX plate reader for 48 hours while shaking. Following the shaking, the liquid media and any planktonic cells were dumped into 10% bleach. Each well was rinsed with 400 µL of H₂O and dumped again into the bleach. The plate was incubated at 37° for 10-20 mins or until dry. Next, 250 µL of 1% crystal violet was added to each well and was incubated at room temperature for 10 minutes to stain the biofilm. The 1% crystal violet solution was dumped, and the plate was submerged in water three times to remove as much stain as possible. The plate was dried for 10 minutes at 37° C. Then,

250 μ L 30% acetic acid was added to each well to dissolve the crystal violet. The plate was left to sit at room temperature for 5 minutes. Using the Biotek Synergy HTX plate reader, a single reading at 590 nm was performed (21).

To examine the difference in biofilm formation between wild-type (WT) and the $\Delta yqeK$ mutant both with and without $\text{NO}\cdot$ exposure, the absorbance measurements were analyzed using a two-way ANOVA with a sidak's multiple comparison test in R-studio.

2.4 Human Plasma Biofilm Assay

A modification of the biofilm quantification was later performed which introduced human plasma pre-coating of the 96-well plates to more closely mimic an indwelling device. (22). This previously published biofilm assay was adapted as follows. The TSB growth media was modified to include 0.5% dextrose and 3% sodium chloride (NaCl) to the TSB mixture, based on previous research which demonstrated an increase in biofilm under the presence of dextrose and sodium chloride (23). The human plasma (Sigma Aldrich and concentration or description) was diluted 1:5 with a mixture containing 0.0342 M sodium bicarbonate and 0.0157 M sodium carbonate. While the overnight culture was growing, 250 μ L of the human plasma dilution was pipetted into each well and left to incubate at 4° C for 24 hours. Following incubation, the human plasma mixture was discarded and the bacteria was added (200 μ L/well at an OD₆₅₀ 0.01 as described above). The 96-well plate was incubated, not shaking, for 48 hours with parafilm wrapped around the plate with the lid on to prevent desiccation. The original biofilm assay protocol was followed after the incubation period.

Results

Our first aim was to examine if YqeK plays a role in *S. aureus* $\text{NO}\cdot$ resistance. To examine if growth differences occur in the $\Delta yqeK$ deletion strain relative to WT with and without $\text{NO}\cdot$ stress, a growth curve assay was performed. The bacteria were grown with, or without, the presence of 10 mM of the $\text{NO}\cdot$ donor DETA/ NO , for 24 hours. Following growth, data analysis was performed to quantify the time for each bacterial replicate to reach an OD₆₅₀ of 0.4 as an approximation of lag time (Figure 3). There was no significant difference between WT and $\Delta yqeK$ lag time without the presence of $\text{NO}\cdot$. Under $\text{NO}\cdot$ stress conditions, however, the $\Delta yqeK$ mutant took significantly longer to reach an OD₆₅₀ of 0.4 relative to WT ($p = 0.034$, two-way ANOVA). We also looked at another metric of fitness during the same growth curve experiments: maximum growth rate (over a 15-minute interval) achieved during exponential phase. Under aerobic conditions, there was no significant difference between the $\Delta yqeK$ deletion mutant and WT. In the presence of $\text{NO}\cdot$ however, there was a significant difference in maximum growth rate between $\Delta yqeK$ and WT (Figure 4; $p < 0.0001$).

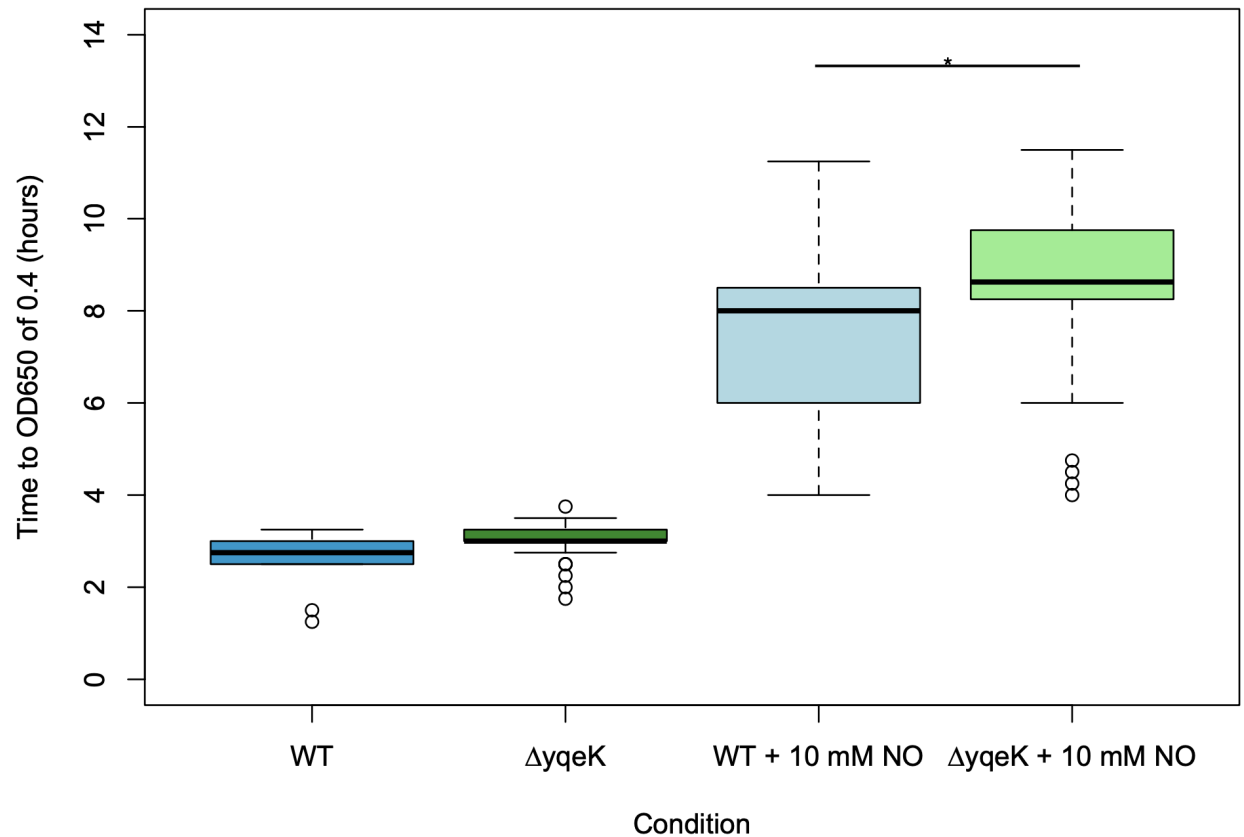


Figure 3. Time required for the bacteria to reach an OD650 (hours). The presence of NO \cdot and *yqeK* both impacted lag time (two-way ANOVA; row factor (strain) $p=0.0094$; column factor (presence/absence NO \cdot) $p < 0.0001$; interaction $p = 0.15$). During NO \cdot stress, $\Delta yqeK$ had a significantly increased lag time relative to WT (Bonferroni's multiple comparisons test * $p < 0.034$).

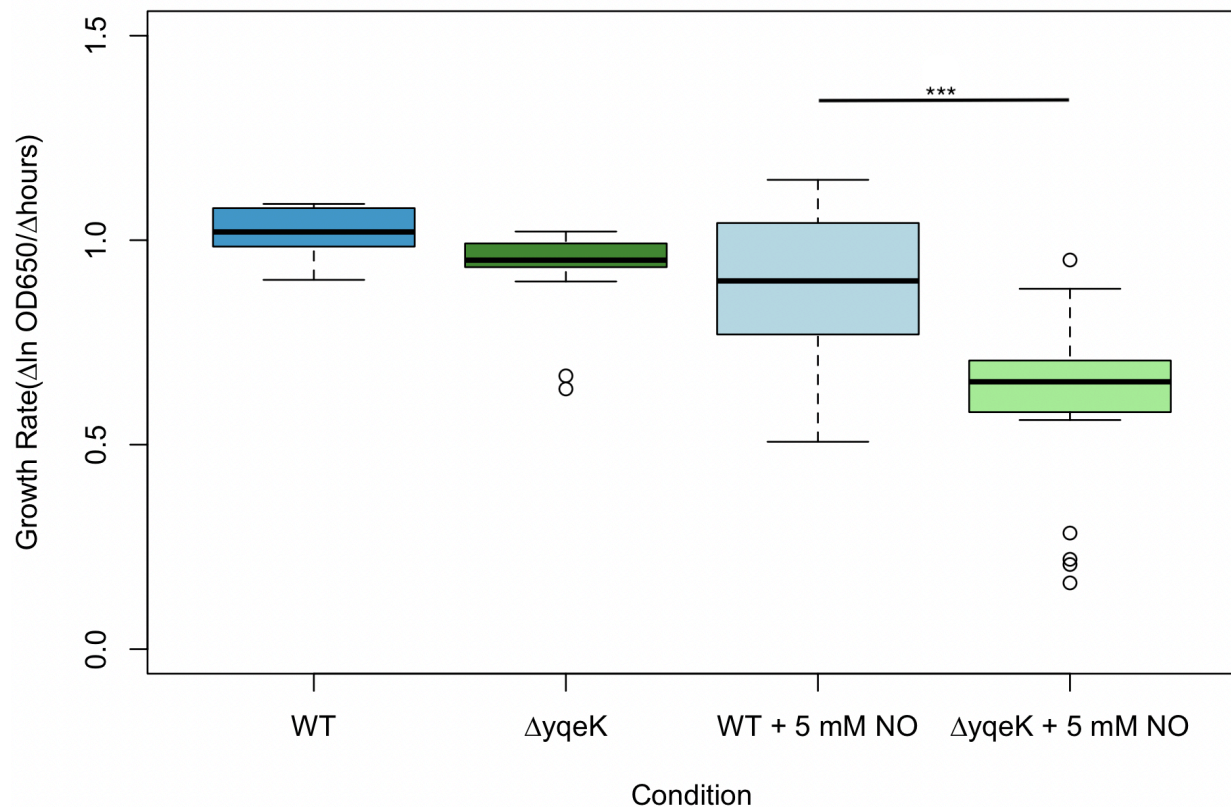


Figure 4. Maximum growth rate (over a 15-minute interval) achieved during exponential phase. The presence of NO^\cdot decreased the maximum growth rate for both the $\Delta yqeK$ and WT strains. The presence of NO^\cdot and the deletion of *yqeK* both impacted growth rate (two-way ANOVA; row factor (strain) $p = 0.0001$; column factor (presence/absence NO^\cdot) $p < 0.0001$; interaction $p=0.031$). Therefore, the presence of YqeK and the presence of NO^\cdot interact to impact growth rate. During NO^\cdot stress, the $\Delta yqeK$ deletion mutant had a significantly reduced max growth rate relative to WT (Bonferroni's multiple comparisons test * $p < 0.0001$).

Because Ap_4A impacts biofilm formation in other species of bacteria (11), our next aim was to examine if biofilm formation was impacted by the deletion of *yqeK*. Previous research found that the addition of NO^\cdot generally increases biofilm formation in *S. aureus*, so we performed biofilm assays both with and without NO^\cdot (24). We performed a 96-well plate crystal violet biofilm assay to assess relative biofilm formation in the WT and $\Delta yqeK$ strains. (Figure 5). There was no significant difference between WT and $\Delta yqeK$ biofilm formation in the absence of NO^\cdot , and biofilm formation was minimal under these conditions. However, there was a significant difference between WT and $\Delta yqeK$ biofilm formation in the presence of 5 mM DETA/ NO^\cdot ($p=0.0004$, two-way ANOVA with Bonferroni's multiple comparison test). Similar to previous research, biofilm formation increased in the presence of NO^\cdot .

Although we detected reduced biofilm formation in the $\Delta yqeK$ deletion mutant relative to WT, overall biofilm formation was very minimal in our assays regardless of the presence of $\text{NO}\cdot$. To increase overall biofilm formation and make the *in vitro* biofilm assay more representative of *in vivo* biofilm conditions, the biofilm assay was repeated with human plasma-coated 96-well plates and using TSB media supplemented with NaCl and dextrose. A similar protocol was followed as the previous biofilm formation assay, with half of the wells receiving 5 mM $\text{NO}\cdot$, to examine the effect of YqeK on biofilm formation in the presence of human plasma proteins (Figure 6). Overall biofilm formation was substantially increased in this assay. There was a significant difference between WT and $\Delta yqeK$ biofilm formation in the presence of 5 mM $\text{NO}\cdot$ ($p=0.007$, two-way ANOVA with Bonferroni's multiple comparisons test). During the experiment, the 48-hour incubation caused nearly half of the replicates to dry out completely. We have adjusted the protocol to include a secondary container and the use of parafilm around the side of the 96-well plate to prevent desiccation in the future but more replicates are needed.

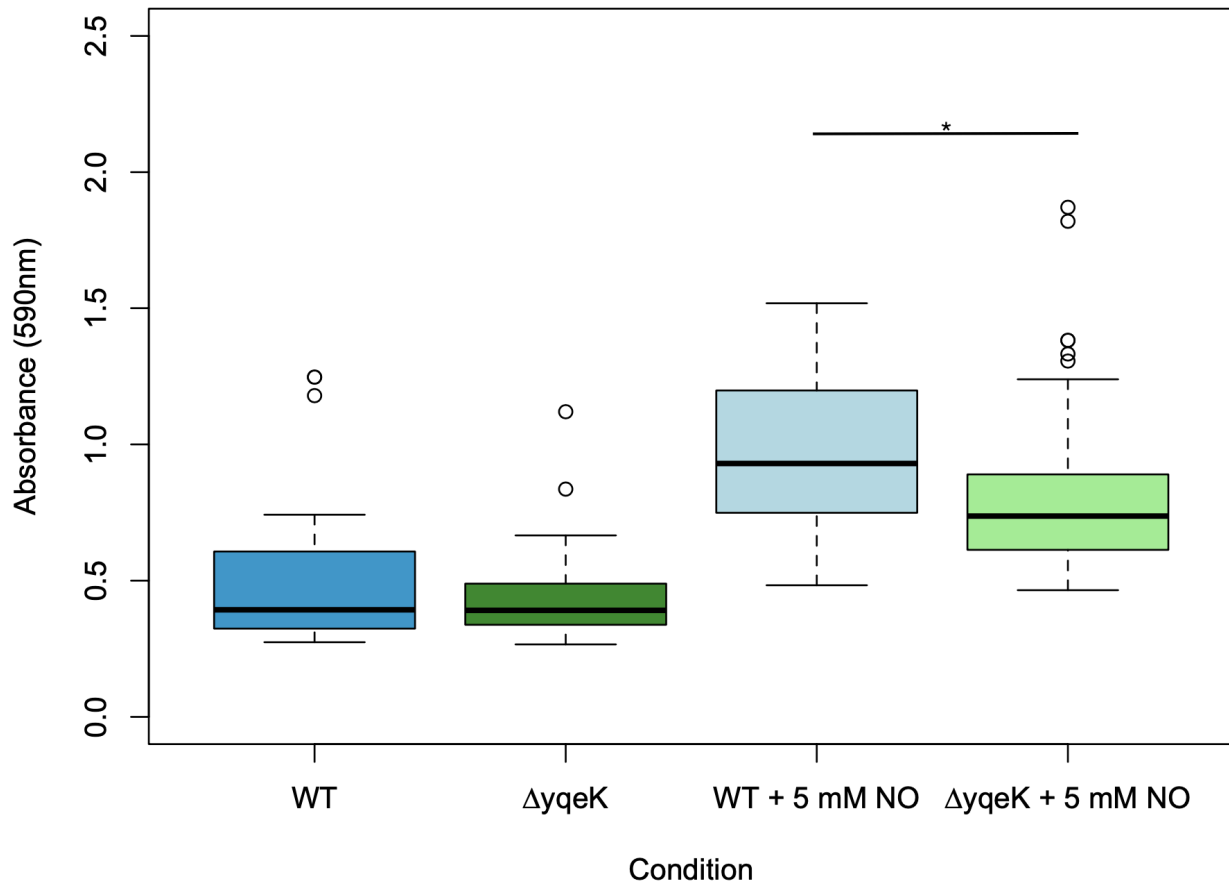


Figure 5. Biofilm formation on a 96-well plate. The presence of $\text{NO}\cdot$ and the deletion of *yqeK* both impacted biofilm formation (two-way ANOVA; row factor (strain) $p=0.0006$; column factor (presence/absence $\text{NO}\cdot$) $p < 0.0001$; interaction $p = 0.064$). During $\text{NO}\cdot$ stress, the $\Delta yqeK$ deletion mutant had a significantly reduced biofilm formation rate relative to WT (Bonferroni's multiple comparisons test $*p = 0.0004$).

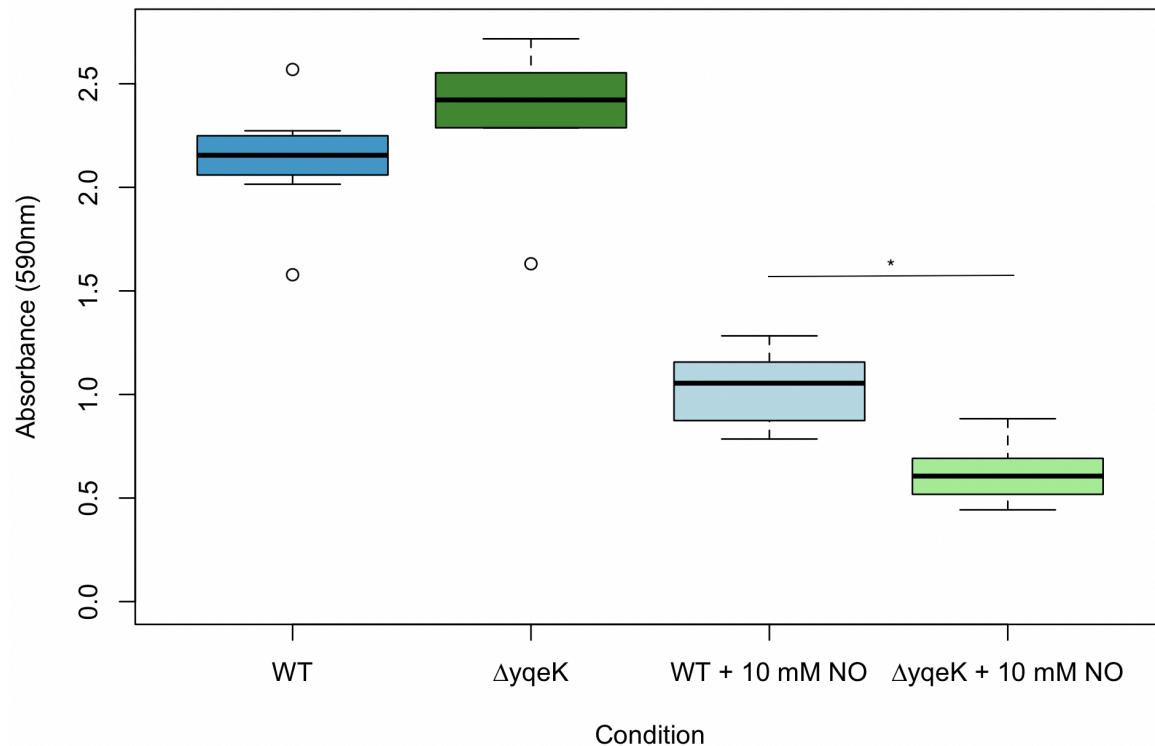


Figure 6. The human plasma biofilm assay demonstrates that the presence of NO^\cdot and the deletion of *yqeK* both impacted biofilm formation (two-way ANOVA; row factor (strain) $p=0.31$; column factor (presence/absence NO^\cdot) $p<0.0001$; interaction $p=0.001$). Therefore, the presence of YqeK and the presence of NO^\cdot interact to impact biofilm formation. During NO^\cdot stress, the $\Delta yqeK$ deletion mutant had a significantly reduced biofilm formation rate relative to WT (Bonferroni's multiple comparisons test $*p<0.007$).

Discussion

Although the enzymatic function of the *S. aureus* YqeK enzyme as an Ap_4A hydrolase has been demonstrated (11), the role of YqeK (and Ap_4A) in the physiology of *S. aureus* remains a mystery. Here we demonstrate that *yqeK* may serve an important role in *S. aureus* pathogenesis. We examined how the deletion of *yqeK* affected growth rate in the presence of NO^\cdot , and biofilm formation, both on a polystyrene 96-well plate and on a human plasma-coated 96-well plate in the presence of NO^\cdot . Our results indicated that the $\Delta yqeK$ deletion mutant performed worse under NO^\cdot conditions when growth rate and biofilm formation was assessed.

In many other bacteria, Ap_4A builds up in large amounts under oxidative and heat stress, and likely other under conditions. However, it is unknown whether *S. aureus* also builds up Ap_4A under other stressful conditions, and whether an excess of it causes cells to be less resistant to antibiotics and/or form less biofilm (25). In our $\Delta yqeK$ deletion, Ap_4A levels have yet to be determined, but we expect them to be elevated due to the absence of Ap_4A hydrolysis by YqeK. Future studies will include the quantification of Ap_4A levels, using high-performance liquid chromatography (HPLC) and mass

spectroscopy in both the deletion mutant and WT under oxidative stress induced by $\text{NO}\cdot$. The phenotype of the $\Delta yqeK$ mutant is different under nitrosative stress conditions, but confirmations are required before indicating the nature of this difference. High concentrations of Ap_4A are somehow producing a reduced growth rate and biofilm production, therefore, YqeK could be a viable target for antibiotics or adjuvant antibiotics.

Future directions also include RNA-sequencing to quantify overall gene expression under both $\text{NO}\cdot$ stress and no stress in WT and the $\Delta yqeK$ mutant to determine the impact of Ap_4A dysregulation on gene expression. To expand upon the human plasma biofilm assay, a simulated endocardial vegetation model will be used to assess biofilm formation under more realistic life-like conditions with the constant movement of nutrients through the area, in an attempt to emulate conditions resembling biofilm formation on a heart valve, for example. This assay would lead to the most logical conclusion about the role of yqeK on biofilm formation in the body, without using an animal model.

Acknowledgements

This work was supported by an American Heart Association AIREA grant (23AIREA1053493) and by the UNCA Undergraduate Research Program. Also I want to thank my research mentor: Dr. Melinda Grosser, for all of her help and for being an amazing advisor!

References

1. Suaya JA, Mera RM, Cassidy A, O'Hara P, Amrine-Madsen H, Burstin S, et al. 2014. Incidence and cost of hospitalizations associated with *Staphylococcus aureus* skin and soft tissue infections in the United States from 2001 through 2009. *BMC Infect Dis. BioMed Central*; 14: 296.
2. Grosser MR, Weiss A, Shaw LN, Richardson AR. 2016. Regulatory requirements for *Staphylococcus aureus* nitric oxide resistance. *J. Bacteriol.* 198(15):2043-2055.
3. Richardson AR, Dunman PM, Fang FC. 2006. The nitrosative stress response of *Staphylococcus aureus* is required for resistance to innate immunity. *Mol Microbiol* 61:927–939.
4. Foster MW, McMahon TJ, Stamler JS. 2003. S-nitrosylation in health and disease. *Trends in Molecular Medicine*. 9: 160–168.
5. Richardson AR, Payne EC, Younger N, Karlinsey JE, Thomas VC, Becker LA, et al. 2011. Multiple Targets of Nitric Oxide in the Tricarboxylic Acid Cycle of *Salmonella enterica* Serovar Typhimurium. *Cell Host Microbe*. Elsevier Inc; 10: 33–43.
6. David A. Wink, James B. Mitchell,. 1998. Chemical biology of nitric oxide: insights into regulatory, cytotoxic, and cytoprotective mechanisms of nitric oxide, *Free Radical Biology and Medicine*, Volume 25, Issues 4–5, Pages 434-456,
7. Grosser MR, Paluscio E, Thurlow LR, Dillon MM, Cooper VS, Kawula TH, Richardson AR. 2018. Genetic requirements for *Staphylococcus aureus* nitric oxide resistance and virulence. *PLoS Pathogens*. 14(3).
8. Arora DP, Hossain S, Xu Y, Boon EM. 2015. Nitric Oxide Regulation of Bacterial Biofilms. *Biochemistry*. 54(24):3717–3728.
9. Beaume M, Hernandez D, Farinelli L, Deluen C, Linder P, Gaspin C, Romby P, Schrenzel J, Francois P. 2010. Cartography of Methicillin-Resistant *S. aureus* Transcripts: Detection, Orientation and Temporal Expression during Growth Phase and Stress Conditions. DeLeo FR, editor. *PLoS ONE*.
10. Minazzato G, Gasparrini M, Amici A, Cianci M, Mazzola F, Orsomando G, Sorci L, Raffaelli N. 2020. Functional characterization of COG1713 (YqeK) as a novel diadenosine tetraphosphate hydrolase family. *J. Bacteriol.*
11. Monds RD, Newell PD, Wagner JC, Schwartzman JA, Lu W, Rabinowitz, O'toole GA. 2010. Di-Adenosine Tetraphosphate (Ap₄A) Metabolism impacts biofilm

formation by *Pseudomonas fluorescens* via modulation of c-di-GMP-dependent pathways. *J. Bacteriol.* 192(12):3011-3023.

12. Bochner BR, Lee PC, Wilson SW, Cutler CW, Ames BN. 1984. AppppA and related adenylate nucleotides are synthesized as a consequence of oxidation stress. *Cell.* 37:225-232
13. Ferguson F, McLennan AG, Urbaniak MD, Jones NJ, Copeland NA. 2020. Re-evaluation of Diadenosine Tetraphosphate (Ap₄A) From a Stress Metabolite to Bona Fide Secondary Messenger. *Frontiers in Molecular Biosciences.* 7:332.
14. Potuznik JF, Nešuta O, Škríba A, Volenikova B, Mititelu M-B, Mancini F, Serianni V, Fernandez H, Spustova K, Trylcova J, et al. 2023. Diadenosine tetraphosphate (Ap₄A) serves as a 5' RNA cap in mammalian cells. *Angewandte Chemie (Weinheim an der Bergstrasse, Germany).*
15. Wang QH, Hu WX, Gao W, Bi RC. 2006. Crystal structure of the diadenosine tetraphosphate hydrolase from *Shigella flexneri* 2a. *Proteins* 65:1032–1035.
16. Ismail TM, Hart A, McLennan AG. 2003. Regulation of dinucleoside polyphosphate pools by the YgdP and ApaH hydrolases is essential for the ability of *Salmonella enterica* serovar typhimurium to invade cultured mammalian cells. *J. Biol. Chem.* 278(35):32602-32607.
17. Cartwright JL, Britton P, Minnick MF, McLennan MF. 1999. The *lalA* invasion gene of *Bartonella bacilliformis* encodes a (de)nucleoside polyphosphate hydrolase of the MutT motif family and has homologs in other invasive bacteria. *Biochem. Biophys. Res. Commun.* 256(3):474-479.
18. Monds RD, Newell PD, Wagner JC, Schwartzman JA, Lu W, Rabinowitz JD, O'Toole GA. 2010. Di-adenosine tetraphosphate (Ap₄A) metabolism impacts biofilm formation by *Pseudomonas fluorescens* via modulation of c-di-GMP-dependent pathways. *J Bacteriol* 192:3011–3023.
19. Zheng T, Jing M, Gong T, Yan J, Zeng J, Li Y. 2021. Deletion of the *yqeK* gene leads to the accumulation of Ap₄A and reduced biofilm formation in *Streptococcus mutans*. *Molecular oral microbiology.* 37(1):9–21.
20. Vitko NP, Richardson AR. 2013. Laboratory maintenance of methicillin-resistant *staphylococcus aureus* (MRSA). *Current Protocols in Microbiology.* 28(1).
21. O'Toole GA. 2011 Microtiter dish biofilm formation assay. *J Vis Exp.* (47):2437.

22. Beenken KE, Blevins JS, Smeltzer MS. 2003. Mutation of sarA in *Staphylococcus aureus* Limits Biofilm Formation. *Infection and Immunity*. 71(7):4206–4211.
23. Götz F. *Staphylococcus* and biofilms. 2002 *Mol Microbiol*. Mar;43(6):1367-78.
24. Plate L, Marletta MA. 2012. Nitric oxide modulates bacterial biofilm formation through a multicomponent cyclic-di-GMP signaling network. *Mol Cell*. May 25;46(4):449-60.
25. Giammarinaro, PI. 2023. *Molecular Mechanisms of Alarmones During Bacterial Stress Responses*. Philipps-Universität Marburg.